

SUPERDENSE MASSIVE GALAXIES IN THE NEARBY UNIVERSE

IGNACIO TRUJILLO¹, A. JAVIER CENARRO, ADRIANA DE LORENZO-CÁCERES, ALEXANDRE VAZDEKIS, IGNACIO G. DE LA ROSA,
 AND ANTONIO CAVA

Instituto de Astrofísica de Canarias, E-38205 La Laguna, Tenerife, Spain; trujillo@iac.es
 Received 2008 October 28; accepted 2009 January 13; published 2009 February 6

ABSTRACT

Superdense massive galaxies ($r_e \sim 1$ kpc; $M \sim 10^{11} M_\odot$) were common in the early universe ($z \gtrsim 1.5$). Within some hierarchical merging scenarios, a non-negligible fraction (1%–10%) of these galaxies is expected to survive since that epoch, retaining their compactness and presenting old stellar populations in the present universe. Using the NYU Value-Added Galaxy Catalog from the Sloan Digital Sky Survey Data Release 6, we find only a tiny fraction of galaxies ($\sim 0.03\%$) with $r_e \lesssim 1.5$ kpc and $M_\star \gtrsim 8 \times 10^{10} M_\odot$ in the local universe ($z < 0.2$). Surprisingly, they are relatively young (~ 2 Gyr) and metal-rich ($[Z/H] \sim 0.2$). The consequences of these findings within the current two competing size evolution scenarios for the most massive galaxies (“dry” mergers vs. “puffing up” due to quasar activity) are discussed.

Key words: galaxies: evolution – galaxies: formation – galaxies: fundamental parameters – galaxies: peculiar – galaxies: photometry – galaxies: structure

1. INTRODUCTION

The discovery (Daddi et al. 2005; Trujillo et al. 2006) that the most massive galaxies ($M_\star \gtrsim 10^{11} M_\odot$), independently of their star formation rate (Pérez-González et al. 2008), were much more compact in the past (a factor of ~ 4 at $z \gtrsim 1.5$ than their equally massive local counterparts; Trujillo et al. 2007; Longhetti et al. 2007; Zirm et al. 2007; Toft et al. 2007; Cimatti et al. 2008; van Dokkum et al. 2008; Buitrago et al. 2008; van der Wel et al. 2008) forces us to face the question of how these high- z galaxies have evolved into the present-day massive population. Most of the current theoretical work in this area suggests “dry” mergers as the dominant mechanism for the size and stellar mass growth of these very dense galaxies (Khochfar & Silk 2006; Hopkins et al. 2008). As cosmic time evolves, the high- z compact galaxies are thought to evolve into the present-day cores of the brightest cluster galaxies. However, a fraction of these objects might survive intact from early formation having stellar populations with old ages. In fact, in some model renditions, the fraction of massive objects that could last without having any significant transformation since $z \gtrsim 2$ could reach 1%–10% (with a space density of $\sim 10^{-4} \text{ Mpc}^{-3}$; Hopkins et al. 2008). Recently, however, Fan et al. (2008) have suggested an alternative scenario where the size evolution is related to the quasar feedback instead of merging. In this model, galaxies puff up after losing huge amounts of cold gas due to the quasar activity.

If the relic superdense massive galaxies exist in the nearby universe ($z \lesssim 0.2$), we should be able to find several thousands in the Sloan Digital Sky Survey Data Release 6 (SDSS DR6) spectroscopy survey which covers 6750 deg^2 (or a total volume of $3.73 \times 10^8 \text{ Mpc}^3$ up to $z = 0.2$). With this aim, we have used the NYU Value-Added Galaxy Catalog (Blanton et al. 2005b) to probe whether there is any nearby massive ($M_\star \sim 10^{11} M_\odot$) galaxy as compact ($r_e \sim 1$ kpc) as those found at high z , and if so, study their stellar populations to provide unique clues for understanding the nature and evolution of these objects. In what follows, we adopt a cosmology of $\Omega_m = 0.3$, $\Omega_\Lambda = 0.7$, and $H_0 = 70 \text{ km s}^{-1} \text{ Mpc}^{-1}$.

2. THE DATA

Our sample was selected using the NYU Value-Added Galaxy Catalog (DR6).² This catalog includes photometric information for a total of $\sim 2.65 \times 10^6$ nearby (mostly below $z \sim 0.3$) objects. Around 1.1×10^6 of these objects have spectroscopic redshift determination. In addition, the catalog contains information about effective radii (Blanton et al. 2005a) and stellar masses (Blanton & Roweis 2007) based on a Chabrier (2003) initial mass function (IMF).

With $0 < z < 0.2$ and $M_\star > 8 \times 10^{10} M_\odot$, there are 152,083 targets. From these, 253 objects ($\sim 0.17\%$ of the above subsample) have $r_e < 1.5$ kpc according to the catalog. 56 of these objects are likely to be point sources (i.e., stars) since their size estimates in the r band are smaller than $0''.05$ and are not considered in what follows. This left a total number of 197 targets ($\sim 0.13\%$). As expected because of their compact nature, the vast majority of these objects are QSOs (146) with a tiny contamination of stars (3) according to the SDSS classification spectra, and are not considered in our analysis since their sizes are not representative of their host galaxies. After a detailed visual inspection of the remaining set of objects (48; i.e., only 0.03% of our initial subsample), we find that three are very close to very bright stars, eight are in close pairs with other galaxies, and eight are edge-on disk galaxies where dust effects can be relevant, preventing us from using them for a further analysis. Consequently, we remain with a final selection of 29 galaxies (see Table 1). The mean redshift of these galaxies is ~ 0.16 with an rms of 0.02. These objects have a mean effective radius of ~ 1.3 kpc (rms 0.15 kpc) and a mean stellar mass of $\sim 9.2 \times 10^{10} M_\odot$ (rms $1.2 \times 10^{10} M_\odot$). Assuming a spherical symmetry, this implies a stellar density of $\sim 5 \times 10^9 M_\odot \text{ kpc}^{-3}$ (this is just a factor of ~ 2 smaller than some globular clusters) and a stellar surface mass density of $\sigma_{50} \sim 9 \times 10^9 M_\odot \text{ kpc}^{-2}$. Figure 1 illustrates the position of the selected compact galaxies in the stellar mass–size plane, as well as some examples of the galaxies in our sample.

¹ Ramón y Cajal Fellow.

² <http://sdss.physics.nyu.edu/vagc-dr6/vagc0/>.

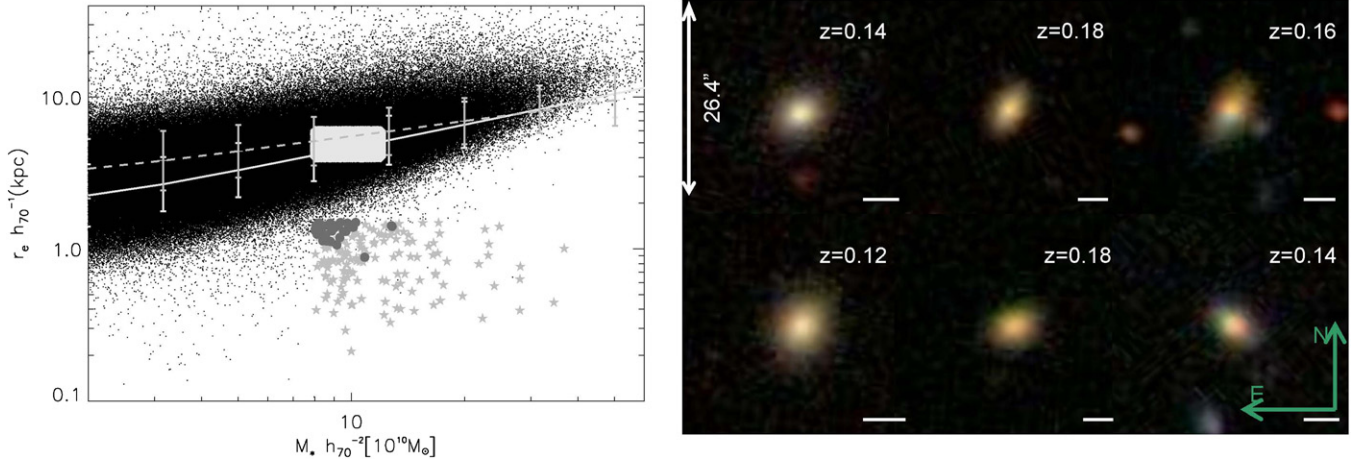


Figure 1. Left: stellar mass–size distribution of the NYU Value-Added Galaxy Catalog (DR6) galaxies. The position of our sample of compact galaxies is shown with circles. The stars are sources that according to the SDSS spectra classification are QSOs. Following Shen et al. (2003), overplotted on the observed distribution are the mean and dispersion of the distribution of the Sérsic half-light radius of the SDSS early-type ($n > 2.5$; solid line) and late-type ($n < 2.5$; dashed line) galaxies as a function of the stellar mass. The gray rectangular area shows the region used to extract the control sample galaxies. Right: mosaic showing six typical galaxies from our sample. The solid lines indicate the equivalent to 10 kpc size at the distance of the objects.

Table 1
Superdense Massive Galaxies Sample

ID NYU	Name	R.A. (J2000)	Decl. (J2000)	M_* ($10^{10} M_\odot$)	r_e (kpc)	Redshift
54829	SDSS J153019.45–002918.6	232.58104	−0.4885095	8.39	1.12	0.085
155310	SDSS J122705.10–031317.9	186.77130	−3.2216436	9.31	1.18	0.165
225402	SDSS J113019.87+664928.8	172.58281	66.824716	9.67	1.30	0.143
265845	SDSS J120032.46+032554.1	180.13528	3.4317179	8.01	1.31	0.143
321479	SDSS J212052.74+110713.1	320.21978	11.120310	10.10	1.38	0.128
411130	SDSS J082927.82+461331.4	127.36594	46.225414	8.86	1.30	0.167
415405	SDSS J103050.53+625859.8	157.71053	62.983350	8.61	1.42	0.167
417973	SDSS J090324.19+022645.3	135.85081	2.4459195	12.82	1.40	0.187
460843	SDSS J143612.56+040411.8	219.05236	4.0699679	8.58	1.12	0.152
685469	SDSS J222140.32+135914.2	335.41803	13.987279	9.03	1.38	0.149
721837	SDSS J111136.18+534011.9	167.90070	53.670063	8.54	1.23	0.142
796740	SDSS J144736.37+432945.7	221.90155	43.496021	9.76	1.47	0.182
807147	SDSS J095705.52+045107.0	149.27301	4.8519610	8.78	1.47	0.162
815852	SDSS J100629.34+071406.4	151.62225	7.2351152	9.35	1.49	0.121
824795	SDSS J105324.14+062421.2	163.35062	6.4058952	10.26	1.49	0.186
890167	SDSS J153934.07+441752.2	234.89197	44.297863	8.79	1.11	0.143
896687	SDSS J143547.19+543528.7	218.94667	54.591381	9.23	1.43	0.130
929051	SDSS J091926.44+065321.4	139.86017	6.8892928	8.25	1.44	0.184
986020	SDSS J083917.44+303745.8	129.82268	30.629409	9.51	1.30	0.179
1044397	SDSS J101637.23+390203.6	154.15510	39.034329	10.84	0.88	0.195
1173134	SDSS J123238.80+425120.6	188.16165	42.855720	8.31	1.35	0.166
1689914	SDSS J031406.38+001023.0	48.526604	0.1730749	8.95	1.35	0.163
1780650	SDSS J120251.13+381644.2	180.71304	38.278960	8.23	1.47	0.157
1791371	SDSS J120554.69+400958.9	181.47790	40.166362	9.14	1.06	0.154
1859261	SDSS J091534.74+255606.2	138.89477	25.935065	8.10	1.24	0.155
2174994	SDSS J235202.68+000244.2	358.01117	0.0456248	8.16	1.47	0.193
2258945	SDSS J092723.34+215604.8	141.84726	21.934668	12.77	1.42	0.167
2402259	SDSS J115032.32+170303.5	177.63473	17.050980	8.04	1.41	0.155
2434587	SDSS J111659.35+170917.3	169.24737	17.154811	8.37	1.25	0.172

2.1. Robustness of Stellar Mass and Size Estimates

To address the robustness of the stellar mass and the sizes of the 29 compact galaxies of our sample, we have remeasured these quantities using different codes than those employed in the NYU Value-Added Galaxy Catalog. To check the sizes, we used GALFIT (Peng et al. 2002). To calculate r_e , we used a Sérsic two-dimensional model convolved with the point-spread function of the image (obtained from a nearby star to the source). After circularizing the GALFIT sizes we find a good

agreement between both estimates, the GALFIT measurement being marginally smaller: $\Delta r_e/r_e = -0.17 \pm 0.14$. The Sérsic indices are also very similar using both codes: $\Delta n/n = -0.04 \pm 0.21$, and with $\langle n \rangle \sim 4.7$. In addition, to check whether our galaxies can be affected by a potential bias due to a recent central burst which resulted in an underestimation of our sizes, we have compared the sizes found in the r band against the sizes measured in the other SDSS filters (u , g , i , and z). In all the bands, the galaxies show very similar sizes.

If anything, the galaxies are slightly larger in the u band (i.e., against the hypothesis of a central starburst): $\langle (r_{e,r} - r_{e,u}) / r_{e,r} \rangle = -0.19 \pm 0.07$, although the result is not statistically significant.

The stellar masses were remeasured using the Bell et al. (2003) prescription based on the rest-frame $(g - r)$ color assuming a Kroupa IMF. We obtain a very good agreement with the NYU Value-Added Galaxy Catalog estimates: $\Delta M_*/M_* = 0.02 \pm 0.08$. In addition to the stellar masses, we have compiled the central velocity dispersions of these objects provided by the SDSS archive. We get a median central velocity dispersion of 196 km s^{-1} with a standard deviation of 30 km s^{-1} . We have also checked these values using the Penalized Pixel-Fitting method developed by Cappellari & Emsellem (2004), and we find an excellent agreement with the SDSS measurements: $\Delta\sigma/\sigma = 0.00 \pm 0.07$.

2.2. Control Sample

In order to make a consistent analysis of the stellar population properties of the compact galaxies we have created, using the same catalog, a control sample of galaxies with similar stellar masses but with sizes representative of the average galaxy population. These galaxies were selected using the following criteria: $0.8 < M_* < 1.2 \times 10^{11} M_\odot$, $4 < r_e < 6 \text{ kpc}$, and within a volume of radius 30 Mpc in relation to the compact galaxies (to assure the environmental conditions are similar). This produces a control sample of 299 objects after rejection of galaxies closer to bright stars and undergoing mergers. The control sample shows a median central velocity dispersion of 180 km s^{-1} with a standard deviation of 34 km s^{-1} , and a Sérsic index $\langle n \rangle \sim 3.8$. Interestingly, the mean central velocity dispersion of the control sample is slightly smaller than the mean central velocity dispersion of the compact sample. This trend toward larger central velocity dispersion, at a given fixed mass (luminosity), for those galaxies with smaller sizes is also found in Bernardi et al. (2006).

2.3. SDSS Spectra

The stellar population properties of our sample were analyzed using the spectra available in the SDSS archive. The SDSS spectra cover $3800 < \lambda < 9200 \text{ Å}$ and the fiber has $3''$ diameter. This implies that for a typical compact object of our sample we cover the inner $3r_e$ with a signal-to-noise ratio (S/N) of ~ 30 . A stacked spectrum of the galaxies in our sample is shown in Figure 2. We also show the stacked spectrum of the galaxies in our control sample. For a typical galaxy in this control sample, the fiber covers the inner $1r_e$ with an S/N ~ 20 .

2.4. AGNs

A potential source of error in the size determination of any galaxy is the presence of an active galactic nucleus (AGN) in its center which can bias our measurements toward smaller sizes. To address this issue, we have estimated which fraction of our compact galaxies are potential AGNs. Following Kauffmann et al. (2003), we have used the BPT diagram (Baldwin et al. 1981) $\log([\text{O III}]/\text{H}\beta)$ versus $\log([\text{N II}]/\text{H}\alpha)$ to identify the AGNs in our sample. Emission line fluxes of $[\text{O III}]$, $\text{H}\beta$, $[\text{N II}]$, and $\text{H}\alpha$ are measured by fitting small regions of the spectrum with width $< 500 \text{ Å}$ around the desired lines. The spectral region is fitted using a linear combination of a Gaussian (to model the emission line) plus ~ 40 stellar population models for the stellar absorption spectra. Based on the MILES stellar library (Sánchez-Blázquez et al 2006; Cenarro et al 2007), these

models are an extension of those in Vazdekis (1999; hereafter V99+). Only objects where the four emission lines are detected with $\text{S/N} > 3$ are considered. We use the demarcation to separate between AGNs and starbursts proposed by Kauffmann et al. (2003; their Equation (1)). On doing this, we find only two galaxies in the compact sample that could be considered as AGNs. Consequently, the fraction of AGN galaxies in our sample is very low ($\sim 7\%$) and our results are not altered by them. Following the same criteria, we find that the number of AGN objects in the control sample is 29 (i.e., $\sim 10\%$), similar to the fraction found in the compact sample. This result reinforces the idea that the presence of an AGN is not affecting our size estimates.

3. STELLAR POPULATIONS

To investigate whether the distinct structural properties of both samples of galaxies are linked to differences in their stellar population properties, we have analyzed both their global spectra (Figure 2) and their luminosity-weighted ages and metallicities on the basis of key absorption line-strength indices and stellar population models.

Figure 2 shows that the average compact galaxy looks clearly younger than the average control galaxy. This is well seen from its bluer continuum and from the fact that its $\text{H}\beta$ absorption line is much stronger. Consequently, the metal lines of the compact galaxies are weaker than those found in the galaxies of the control sample. A more detailed disentangling of age and metallicity effects is presented in Figure 3. This figure shows the indices $\text{H}\beta_0$ —an optimized age indicator by Cervantes & Vazdekis (2009)—and $[\text{MgFe}]$ —mainly sensitive to overall metallicity (González 1993)—measured for the compact (filled squares) and control galaxies (dots). All galaxies in the range $0.132 \lesssim z \lesssim 0.159$, with $\text{H}\beta_0$ values likely to be affected by strong $\lambda 5577 \text{ Å}$ $[\text{O I}]$ skyline residuals, have been rejected from the figure and subsequent analysis. To avoid systematics among the galaxy indices due to different velocity dispersions, all the galaxy spectra were previously broadened to match the largest σ value of the whole sample, which is 320 km s^{-1} . Thus, taking into account the SDSS instrumental broadening, all the indices in Figure 3 are given at an overall σ of 332 km s^{-1} . Also, V99+ models are overplotted at the same spectral resolution of the data.

Index uncertainties have been measured for each galaxy from the error spectra provided in the SDSS database. The open square and circle in Figure 3 indicate, respectively, error-weighted mean indices for the compact and control galaxy samples. For each of them, error bars in thick lines illustrate the 1σ typical index uncertainties. In turn, thin error bars provide the error-weighted rms standard deviations. The fact that the typical index errors are smaller than their standard deviations seems to indicate that, within each galaxy subsample, there exist certain differences—not explained by errors—among the stellar populations of their individual galaxies. However, these differences are, by far, negligible as compared to those between compact and control galaxies. As already suggested in Figure 2, it is clear from Figure 3 that compact galaxies are much younger ($\sim 2 \text{ Gyr}$) than the control galaxy sample, which is typically old ($\sim 14 \text{ Gyr}$). There are also hints for compact galaxies having higher metallicities ($[\text{Z}/\text{H}] \gtrsim +0.2$) than the control sample, with averaged values slightly below solar.

It is worth noting here that the above age and metallicity results are unlikely to be due to the larger apertures (a factor

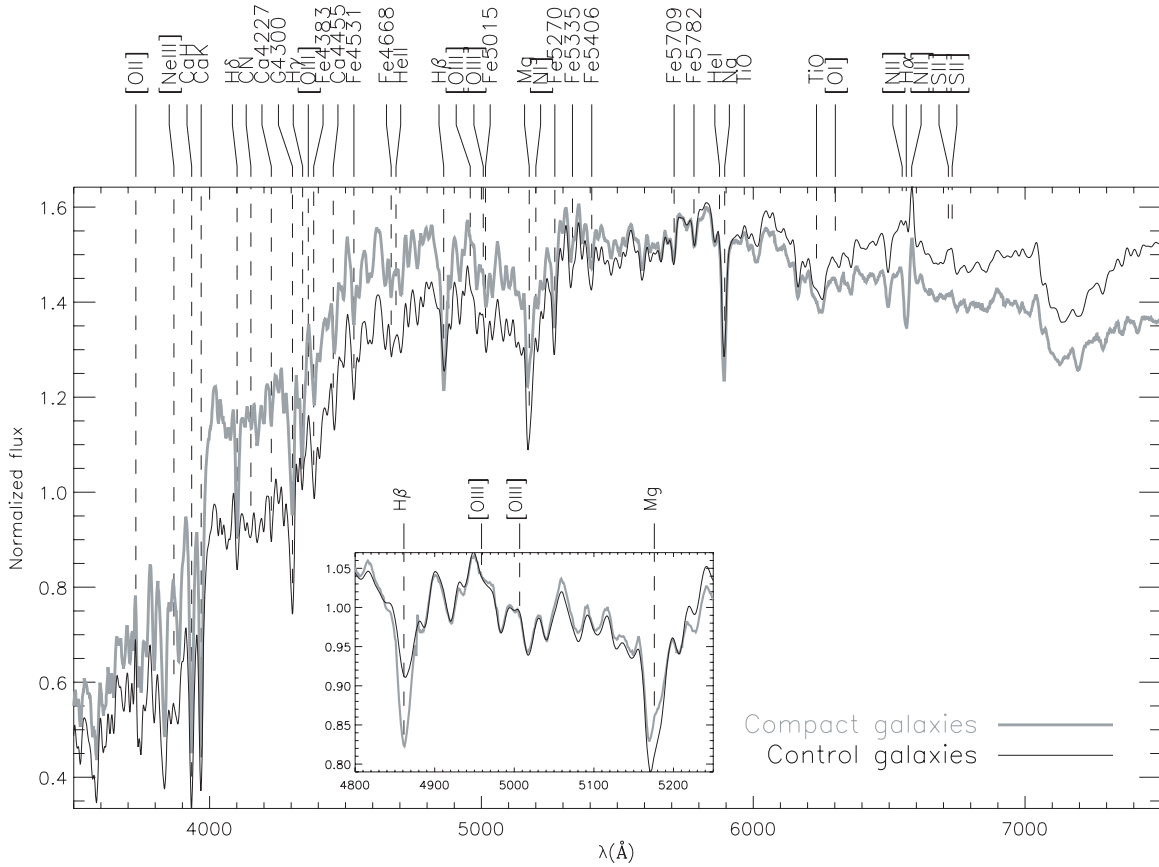


Figure 2. Average mean spectra of the compact galaxies of our sample (gray thick line) and the control galaxies (thin line). The individual spectra were previously convolved to the highest dynamical velocity dispersion (320 km s^{-1}) and divided by their corresponding means, so they contribute with the same weight. Each mean spectrum has been normalized by its mean flux within the spectral range showed in each panel. The inset shows the spectral regions around H β and Mg lines.

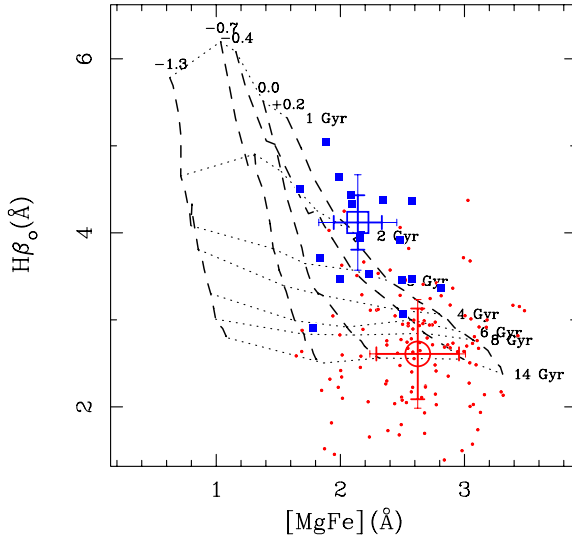


Figure 3. $H\beta_0$ vs. $[MgFe]$ diagram for 151 galaxies of the compact (filled squares, 18) and control samples (dots, 133) for which no $\lambda 5577 \text{ Å}$ [O I] skyline residuals affect the index measurements. Overplotted are V99+ SSP model grids with different ages (dotted lines) and metallicities (dashed lines) as given in the labels. The open square and circle are error-weighted mean indices for the compact and control samples, respectively. Thick error bars show the 1σ index uncertainties, whereas the thin error bars correspond to the dispersions of the samples.

of 3 in units of r_e ; see Section 2.3) sampled for the compact objects, as detailed studies of age and metallicity gradients in

normal ellipticals (e.g., Sánchez-Blázquez et al. 2006) report that their outer parts are, on average, less metal-rich and slightly older than their centers. Therefore, if aperture issues were significantly affecting the stellar population properties of the integrated spectra, we would expect compact objects to be older and more metal poor. Also, note that the total galaxy luminosity within $3r_e$ is (for a Sérsic surface brightness profile with $n = 4$) only 1.6 larger than that within $1r_e$ (Trujillo et al. 2001), so if the outer regions were the clue for the strong differences in luminosity-weighted age between both galaxy subpopulations, compact objects should have unprecedented young populations in their outskirts.

4. DISCUSSION

The surprising young ages of the superdense massive galaxies in the nearby universe cast some doubts about what are the mechanisms that the most massive galaxies in the high-redshift universe follow to reach their current sizes. At high redshift, the most massive galaxies are supposed to be the result of gas-rich mergers resulting in a compact remnant (e.g., Khochfar & Silk 2006; Naab et al. 2007). After this, dry mergers are expected to be the mechanism that moves these very massive galaxies toward the current stellar mass–size relation. Within this scheme, a non-negligible fraction (1%–10%) of superdense massive galaxies is expected to survive intact since that epoch (Hopkins et al. 2008) and, consequently, they are supposed to have old stellar populations; this is at odds with our findings. The above survival rate, however, is an upper limit since only major mergers (ratio 1:3) were considered in estimating this

number density in Hopkins et al. (2008). In fact, the role of minor mergers and small accretion can be very relevant (Naab et al. 2007) in explaining the puffing up of galaxies. Within the scheme of the dry merging scenario, our result could highlight the importance of accounting for minor merging in order to make robust estimations of the number density of old superdense massive galaxies in the present universe.

If our compact galaxies are not relics of the early universe how they could be formed? A possibility is that they come from recent gas-rich disks merging. If this is the case, we should not find many in the present-day universe since the current massive disks population has not enough gas. This could explain why the number of superdense young massive galaxies is so scarce in the local universe.

Recently, Fan et al. (2008) have suggested a puffing-up scenario where the superdense massive galaxies in the early universe can grow in size without suffering merging. This mechanism, analogous to the one proposed to explain the growth of globular clusters (Hills 1980), argues that the observed strong evolution in size is related to the quasar feedback, which removes huge amounts of cold gas from the central regions, quenching the star formation. If this mechanism took place in all massive galaxies in the past, no old superdense massive galaxy should be observed today, as seems to be the case. However, against this puffing-up scenario could be the stellar population ages of our galaxies. According to the Fan et al. model, after the quenching of the star formation due to the gas ejection, the galaxy needs some time to reach its new equilibrium configuration. Following their model, the amount of time is about 40 dynamical times. In massive galaxies this will be around 2 Gyr. Interestingly, this is the typical mean luminosity-weighted age of the stellar population of our galaxies. However, we see that they are still very compact. It is not clear how this can be fully accommodated within the Fan et al. scenario.

A key element to explore the size evolution process is to study the evolution of the central velocity dispersion, σ_* , of the most massive galaxies at a given halo mass. The two competing scenarios, “dry mergers” versus “puffing up,” predict a very different evolution of the central velocity dispersion as cosmic time evolves. In the merging scenario, σ_* is basically constant with time, at most a factor of 1.3 higher at high z (Hopkins et al. 2008). In the “puffing-up” scenario, the original (before the expansion of the object) central velocity dispersion depends on formation redshift as $(1 + z_{\text{form}})^{1/2}$. As the object inflates, σ_* changes with the effective radius as $\sigma_* \propto r_e^{-1/2}$. Our results show that galaxies in the control (already “puffed up” in this scenario) and compact samples have very similar σ_* . If both type of objects were formed at high redshift, our results will be in contradiction with the “puffing-up” scenario. If, on the other hand, the nearby superdense massive galaxies have been formed recently, our results agree with that scenario since young, low- z galaxies in the superdense phase should have velocity dispersions similar to old “puffed-up” galaxies, because the effect of the increase of the radius essentially compensates the effect of the different z_{form} .

To test the prediction of the puffing-up scenario is key to knowing whether the nearby superdense massive galaxies are genuinely young objects. We need to constrain whether our relatively young mean luminosity-weighted age estimate of ~ 2 Gyr is representative of the whole stellar population of the objects or an artifact due to a recent burst not involving a large amount of stellar mass. To address this issue, we have probed the star formation history (SFH) of our objects by

means of STARLIGHT (Cid Fernandes et al. 2005) exploring which simple stellar population model combination best fits the observed spectra. Our preliminary results show that SFHs from the compact galaxies are systematically different to those of the control sample. For an average compact galaxy, more than 64% of the luminosity comes from stellar populations younger than 3 Gyr, in contrast to 7% in the control sample. If this were the case, it will indicate that the superdense massive galaxies are genuinely (structurally speaking) young objects. Finally, a significant test to distinguish between the above two competing scenarios will be possible when central velocity dispersions of superdense massive galaxies at high redshift are determined.

I.T. and A.J.C. acknowledge support from the Ramón y Cajal and Juan de la Cierva Programs financed by the Spanish Government. We appreciate the constructive comments of the referee that improved the quality of the manuscript. We thank Ruymán Azzollini for help on estimating the stellar masses and Jose Acosta and Ana Pérez for advice on AGN determination. Lulu Fan helped us to understand some relevant details of his size evolution model. This work has been supported by the Spanish Ministry of Education and Science grant AYA2007-67752-C03-01.

REFERENCES

- Baldwin, J. A., Phillips, M. M., & Terlevich, R. 1981, *PASP*, **93**, 5
- Bell, E. F., McIntosh, D. H., Katz, N., & Weinberg, M. D. 2003, *Ap&SS*, **149**, 289
- Bernardi, M., et al. 2006, *AJ*, **131**, 2018
- Blanton, M. R., Eisenstein, D., Hogg, D. W., Schlegel, D. J., & Brinkmann, J. 2005a, *ApJ*, **629**, 143
- Blanton, M. R., & Roweis, S. 2007, *AJ*, **133**, 734
- Blanton, M. R., et al. 2005b, *AJ*, **129**, 2562
- Buitrago, F., Trujillo, I., Conselice, C. J., Bouwens, R. J., Dickinson, M., & Yan, H. 2008, *ApJ*, **687**, L61
- Cappellari, M., & Emsellem, E. 2004, *PASP*, **116**, 138
- Cenarro, A. J., et al. 2007, *MNRAS*, **374**, 664
- Cervantes, J. L., & Vazdekis, A. 2009, *MNRAS*, **392**, 691
- Chabrier, G. 2003, *PASP*, **115**, 763
- Cid Fernandes, R., Mateus, A., Sodré, L., Stasinska, G., & Gomes, J. M. 2005, *MNRAS*, **358**, 363
- Cimatti, A., et al. 2008, *A&A*, **482**, 21
- Daddi, E., et al. 2005, *ApJ*, **626**, 680
- Fan, L., Lapi, A., de Zotti, G., & Danese, L. 2008, *ApJ*, **689**, L101
- González, J. J. 1993, PhD thesis, Univ. California.
- Hills, J. G. 1980, *ApJ*, **235**, 986
- Hopkins, P. H., Hernquist, L., Cox, T. J., Keres, D., & Wuyts, S. 2008, in press (arXiv:0807.2868)
- Kauffmann, G., et al. 2003, *MNRAS*, **346**, 1055
- Khochfar, S., & Silk, J. 2006, *ApJ*, **648**, L21
- Longhetti, M., et al. 2007, *MNRAS*, **374**, 614
- Naab, T., Johansson, P. H., Ostriker, J. P., & Efstathiou, G. 2007, *ApJ*, **658**, 710
- Peng, C. Y., Ho, L. C., Impey, C. D., & Rix, H.-W. 2002, *AJ*, **124**, 266
- Pérez-González, P. G., Trujillo, I., Barro, G., Gallego, J., Zamorano, J., & Conselice, C. J. 2008, *ApJ*, **687**, 50
- Sánchez-Blázquez, P., Gorgas, J., & Cardiel, N. 2006, *A&A*, **457**, 823
- Sánchez-Blázquez, P., et al. 2006, *MNRAS*, **371**, 703
- Shen, S., Mo, H. J., White, S. D. M., Blanton, M. R., Kauffmann, G., Voges, W., Brinkmann, J., & Csabai, I. 2003, *MNRAS*, **343**, 978
- Toft, S., et al. 2007, *ApJ*, **671**, 285
- Trujillo, I., Conselice, C. J., Bundy, K., Cooper, M. C., Eisenhardt, P., & Ellis, R. 2007, *MNRAS*, **382**, 109
- Trujillo, I., Graham, A. W., & Caon, N. 2001, *MNRAS*, **326**, 869
- Trujillo, I., et al. 2006, *MNRAS*, **373**, L36
- van der Wel, A., Holden, B. P., Zirm, A. W., Franx, M., Rettura, A., Illingworth, G. D., & Ford, H. C. 2008, *ApJ*, **688**, 48
- van Dokkum, P. G., et al. 2008, *ApJ*, **677**, L5
- Vazdekis, A. 1999, *ApJ*, **513**, 224
- Zirm, A. W., et al. 2007, *ApJ*, **656**, 66